https://doi.org/10.5194/tc-2023-35
Preprint. Discussion started: 16 March 2023

The Cryosphere Discussions

Mapping age and basal conditions of ice in the Dome Fuji region, Antarctica, by combining radar internal layer stratigraphy and flow modeling

Zhuo Wang[1,2], Ailsa Chung[3], Daniel Steinhage[1], Frédéric Parrenin[3], Johannes Freitag[3], and Olaf Eisen[1,4]

[1]Alfred-Wegener-Institut, Helmholtz-Zentrum für Polar und Meeresforschung, Bremerhaven, Germany
[2]College of Geo-Exploration and Technology, Jilin University, Changchun, China
[3]Univ. Grenoble Alpes, CNRS, IRD, IGE, Grenoble, France
[4]Department of Geosciences, Universität Bremen, Bremen, Germany

Correspondence: Olaf Eisen (olaf.eisen@awi.de)

Abstract. The Dome Fuji (DF) region in Antarctica is a potential site for an ice core with a record of over one million years. Here, we combine the internal airborne radar stratigraphy with a 1-D model to estimate the age of basal ice in the DF region. The radar data used in the study were collected in a survey during the 2016–2017 Antarctica season. We transfer the newest age–depth scales from the DF ice core to isochrones in the surrounding 500 km × 550 km region through traced radar isochrones. At each point of the survey the 1-D model uses the ages of isochrones to construct the age–depth scale at depths where dated isochrones do not exist, the basal thermal conditions, including the thickness of a potentially present basal layer and surface accumulation rates. Our resulting age distribution and age density suggest that a few promising sites with ice older than 1.5 million years in the DF region might exist. The deduced melt rates and presence of stagnant ice map provides more constraints for finding sites with a cold base. The accumulation rates range from 0.015 to 0.038 m a^{-1} ice equivalent. The numbers of picked isochrones and the timescale of the ice core severely affect the model results according to sensitivity studies. Our study demonstrates it is possible to find the old ice in the DF region, the constraint from deep radar isochrones and a trustworthy timescale could improve the model estimation.

1 Introduction

To understand the Quaternary climate, the progression of glaciations and the carbon cycle, continuous and undisturbed ice-core records back to 1.5 million years BP (before present, present defined as 1950) are crucial (Fischer et al., 2013; Jouzel and Masson-Delmotte, 2010). The mid-Pleistocene transition (MPT), which occurred in the time interval between 1200 ka and 900 ka BP, termed by a switch from more regular 41 ka glacial cycle (1500 to 1200 ka BP) to current 100 ka glacial cycle (Lisiecki and Raymo, 2005), is still not fully understood. CO_2 and other greenhouse gas may have either forced this switch or might have responded to it (Willeit et al., 2019). A direct record of greenhouse gases with atmospheric record covering this period can only be found in Antarctica ice core (Fischer et al., 2013). Moreover, isotopic and chemical records in ice cores of that age can provide additional information on temperature, ice dynamic changes and magnetic reversals, to be analyzed

https://doi.org/10.5194/tc-2023-35
Preprint. Discussion started: 16 March 2023


The Cryosphere Discussions
Open Access
EGU

together with other marine and terrestrial records (Raymo et al., 2006; Raisbeck et al., 2006; Singer and Brown, 2002). Hence, identifying "Oldest Ice" sites in Antarctica is one of the primary challenges for ice-core research.

There is a huge challenge in retrieving continuous records of old ice cores where the oldest ice is compressed in deep layers near the base of the ice sheet. Ice older than one million years could have melted away by reaching the pressure melting point or be disturbed, and thus not feasible for ice-core analyses, because of complicated processes in the basal layer (Van Liefferinge and Pattyn, 2013). As one consortium in the International Partnerships in Ice Core Sciences (IPICS), the European "Beyond EPICA–Oldest Ice" (BE–OI) consortium initiated pre-site surveys in the wider Dome Concordia (DC) and Dome Fuji (DF) regions. Van Liefferinge and Pattyn (2013) evaluated potential sites of million year-old ice in Antarctica considering ice velocity, ice thickness and geothermal heat flow (GHF) based on a thermo-dynamical model. In a follow-up study, Van Liefferinge et al. (2018) focused on more detailed sites for oldest ice in the DF and DC regions leveraging more robust criteria of ice thickness and velocity, and using a metric for the shape of the bed. In the DC region, Young et al. (2017) proposed some old ice targets through high-resolution aerogeophysical surveys, and Parrenin et al. (2017) inferred the age of ice and further identified two target areas where ice older than 1.5 Ma may exist, based on 1-D thermo-mechanical model constrained by radar observations. Lilien et al. (2021) refined the age–depth scale at Little Dome C (LDC), 40 km from the DC site, based on a high-resolution radar survey on the drilling site determined for the Beyond EPICA project. In the Dome A region, Sun et al. (2014) estimated ice age around Kunlun station by applying a three-dimensional, thermomechanically coupled full-Stokes model, which indicated that in the area without basal melting the ice age at 95 % depth could be limited to 1.5 Ma.

The Dome Fuji region is a potential area for holding oldest ice in Antarctica. The DF station and site of two previous ice-core drillings, is located at 77°19′01″ S, 39°42′12″ E (Ageta et al., 1998) at an elevation of 3810 m, with an ice thickness of 3028±15 m (Fujita et al., 1999, 2015), an annual mean air temperature of −54.4°C (Kameda et al., 2009) and an annual accumulation of $\sim$ 24 mm w.e.a^{-1} (Fujita et al., 2011). The first deep ice core at DF, which was drilled from 1995 to 1996, reached 2503.52 m and covered a record back to $\sim$ 340 ka dated by the isotopic δ^{18}O record (Ageta et al., 1998; Watanabe et al., 1999). Kawamura et al. (2007) used O_2/N_2 measurements, a proxy of local summer insolation, to build a new timescale (referred to as DFO-2006). Based on these O_2/N_2 age markers, Parrenin et al. (2007) used a 1-D ice flow model to reconstruct the timescale down to basal ice and accumulation rates (referred to as DFGT-2006). During the austral summers from 2003/04 to 2006/07, the second deep ice core, only 48 m away from the first ice core (Saruya et al., 2022), was finally drilled to a depth of 3035.22 m. It is considered to be very closed to the bedrock (Motoyama, 2007; Motoyama et al., 2021) and the temperature at the bottom of this ice core reached the melting point (Talalay et al., 2020). The Dome Fuji Ice Core Project Members (2017) dated this deep ice core back to $\sim$ 720 ka by synchronising the isotopic δ^{18}O record with that of ice core at DC (AICC2012) and accumulation rates were also deduced from the δ^{18}O record. A timescale which combines DFO-2006 (< 342 ka) and AICC2012 (> 344 ka) was proposed then (referred to as DFO2006+AICC2012). In addition to direct analysis of ice-core proxies, Seddik et al. (2011) simulated the temperature at the ice base and the age at 95 % of the depth with the Continuum-mechanical Anisotropic Flow model in a $\sim$ 200×200 km domain around the DF drill site. Karlsson et al. (2018) presented an updated subglacial topography with a resolution of 10 km in the DF region based on an airborne radar surveys conducted by the

https://doi.org/10.5194/tc-2023-35
Preprint. Discussion started: 16 March 2023

Alfred Wegener Institute, Helmholtz Centre for Polar and Marine Research (AWI), as part of the Beyond EPICA project. They refined some promising oldest ice sites proposed by Van Liefferinge and Pattyn (2013) using the same model. Their updated age estimates suggested three main areas with potential oldest ice candidates in the DF region. Tsutaki et al. (2022) compiled a new ice thickness dataset with a resolution of 0.5 km based on ground-based radar measurements collected by Japanese Antarctic Research Expedition (JARE), to examine roughness and slope of the ice–bed interface, the stress state of the ice and subglacial hydrological conditions in the vicinity of DF and the so-called New Dome Fuji site (NDF), which focused on a smaller region for old ice. Obase et al. (2022) simulated temperature, basal melt rates and age profiles through a 1-D ice flow model, IcIES-2, along the DF-NDF transect.

Despite of all these progresses, age estimates and basal thermal condition in the larger DF region (i.e. roughly a 500 km × 550 km perimeter) are not yet constrained by isochrones detected by radar. Here, we connect the ice-internal isochrone stratigraphy in the larger DF region to the DF drill site through isochrones traced in the airborne radar data collected during the 2016–17 survey conducted by AWI. We apply a 1-D ice flow model (see more details of the model in the companion paper of Chung et al. (submitted)) to model the age–depth scale below the available isochrone stratigraphy, accumulation rates and also to derive either melt rates or the thickness of a (potentially stagnant) basal layer of ice in the DF region. We finally discuss the reliability of the results, conduct sensitivity experiments to quantify the effect of picked isochrones numbers and the timescale of the ice core on our age estimates as well as the other modeling results.

2 Data and Methods

2.1 Data collection

We use data collected with the airborne radio-echo sounding (RES) system of the AWI mounted on its Basler BT-67 aircraft during the 2016/17 Antarctic season. The radar survey was conducted in the DF region, from a temporary camp (79° S, 30° E) 290 km away from the DF station, where 26 radar profiles were recorded. Survey lines have parallel line spacing of 10 km in the northern part of the study area and 15 km line spacing in the southern part, the spacing distance is getting much smaller when approaching and leaving the camp (Karlsson et al., 2018). In our study we include 22 survey profiles with lengths varying from 622 km to 898 km. The study area covers a region of about 270,000 km^2 and an elevation range of about 3400 m–3810 m (Fig. 1).

The AWI RES system transmits radar waves with a center frequency of 150 MHz and an amplitude of 1.6 kW. During the survey it only operated with the 600 ns long pulse, thus effectively operating as a pulse-limited radar. The theoretical vertical resolution in ice for the 600 ns burst is 50 m (Nixdorf et al., 1999). In this study we use radar returns of the 600 ns long burst from internal reflection horizons (IRHs) as well as from the ice–bedrock interface. The radar data has a mean spacing of 5 m along the flight line (which varies with real speed and direction of aircraft) and is sampled at an interval of 4 ns (Karlsson et al., 2018).

Before picking the IRHs and ice–bed interface, the radar data are resampled to 12 ns and stacked 7 fold, which lead to a mean trace spacing of $\sim$ 35 m. In addition, a low-pass filter and a two-dimension filter are used to decrease noise. Automatic

https://doi.org/10.5194/tc-2023-35
Preprint. Discussion started: 16 March 2023

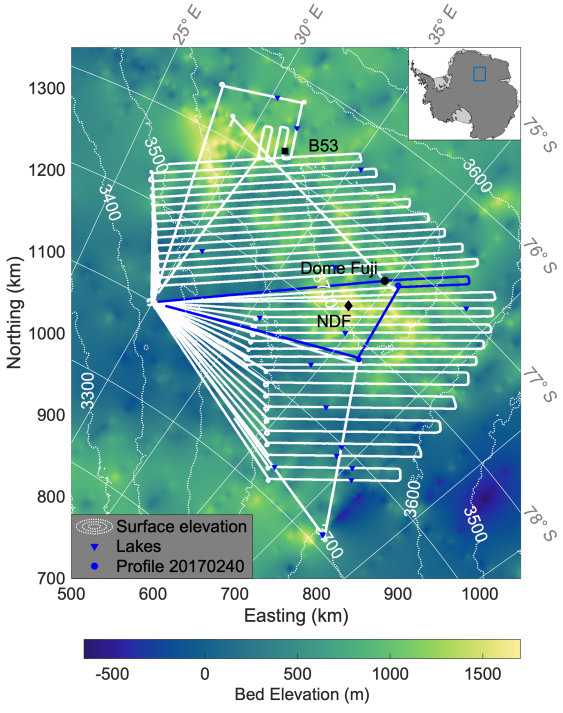

Figure 1. Study area in the DF region, with inset showing the position in Antarctica. The white lines represent radar survey profiles used in our study. The blue line shows the exemplary profile 20170240. We use surface elevation (contour map) and bed elevation from Greene et al. (2017) and Morlighem et al. (2017, 2020). Subglacial lakes were identified by Karlsson et al. (2018).

gain control (AGC) is used to balance the gain and facilitate layer tracing. Processing is performed in the seismic environment of the Echos software from Paradigm Geophysical.

2.2 Horizons picking and dating

In order to provide age markers (i.e., the age of IRHs) and ice thickness to use as observations in our 1-D flow model, IRHs are traced in the two-way travel time (TWT) domain. The surface reflection is picked automatically in Echos and then subtracted in all traces to shift the first break of the radar data to time zero. The maximum reflection power of IRHs is traced manually in the seismic software package Section, which allows IRHs to be continuously traced in different radar profiles through intersections between profiles. This ensures that the same isochronous horizons are traced. We trace 6 or 7 relatively distinct and continuous IRHs (H1–H7) in all survey lines, the third IRH H3 is not clear and continuous enough to be traced in some profiles. Ice–bed returns were picked by Karlsson et al. (2018) through semi-automatic detection routines in Matlab. The ice–bed returns are often diffuse events, especially around mountain peaks, which results in disagreements when using different methods to trace ice–bed returns, and thus differences in ice thickness and modeling results. We emphasize that Karlsson et al. (2018) picked the

https://doi.org/10.5194/tc-2023-35
Preprint. Discussion started: 16 March 2023

first (uppermost) ice–bed return when there were uncertainties, so that ice thickness estimates can be considered a minimum ice thickness in some places.

TWT is converted to depth assuming a constant radar wave speed of 168.5 m μs^{-1} in ice (Winter et al., 2017; Lilien et al., 2021) and a 15.5 m firn correction calculated from depth-density curve in the B53 ice core. The B53 ice core was drilled to 202 m by the AWI team, and is located at 79°47′38″ S, 31°54′19″ E, and ∼ 203.5 km away from the DF drill site (Fig. 1). The point of closest approach on our radar profiles is located ∼ 91.1 m away from the DF drill site, at 77°19′ S, 39°41′59″ E, on the profile 20170240. Ice thickness at this closest point observed from radargram is about 3044.8 m, and the ice thickness in the DF drill site interpolated from radar observations is about 3050.5 m. This corresponds with a previously inferred ice thickness of 3028±15 m from a radar observation (Fujita et al., 1999), and it approximates the depth of the second DF deep ice core, 3035.2 m, which is considered to be very close to ice–bed interface (Motoyama, 2007).

IRHs at this location closest to the DF drill site are firstly converted to depth and then dated by vertical interpolation of the ages from the DFO2006+AICC2012 timescale (Dome Fuji Ice Core Project Members, 2017), available to a depth of 3031 m with an ice age of 715.9 ka BP, and then transferred to the radargram at the depths of the IRHs. Fig. 2 shows traced IRHs H1–H7 in the profile 20170240 with the point of closest approach shown as white vertical line. The age of IRHs, ranging from 31.4 ka (H1) to 169.1 ka (H7), and their age uncertainty, are marked in Fig. 2. Ages of different IRHs are then transferred to all profiles, which then serve as the primary input to the 1-D model.

2.3 Age uncertainty of internal reflection horizons

The uncertainty of IRH age estimates directly impact the reliability of the results from the model, as it includes uncertainty of ice-core agescale and age uncertainty caused by depth uncertainty of IRHs. As for the depth uncertainty of IRHs, we consider slope-induced uncertainty caused by the offset of the closest radargram to the DF drill site, uncertainty of firn correction, uncertainty of dielectric constant of ice and the range precision of the estimate in determining depth (Cavitte et al., 2016). The slope of each IRH varies from 1 m km^{-1} to 14.7 m km^{-1}, which results in a corresponding uncertainty from 0.1 m to 1.5 m for the 91.1 m offset (the distance between the DF drill site and the closest approach on the radar profile). For the firn correction, we used AWI's ICE-CT system to measure the density–depth profile in the upper 126 m of the B53 ice core, with an observational error up to 1 % (Freitag et al., 2013), which results in an uncertainty of 0.5 m in the firn correction. The depth uncertainty of dielectric constant affected by anisotropy and temperature is taken to be 1 % (Lilien et al., 2021). The estimate of the range precision is always higher than the resolution (50 m for AWI RES system) for distinct IRHs. It is determined by the pulse width of the radar waveform, the signal-to-noise ratio and the sub-resolution reflector fluctuations (Cavitte et al., 2016). Our best guess for uncertainty for each IRH is based on continuity and definition during manually tracing, from 20 m to 50 m. Thus, the depth uncertainty varies from 28.5 m to 70.5 m in total, leading to an age uncertainty range from 2.1 ka to 16.8 ka. The age uncertainty of the ice-core itself is interpolated from the age errors of the agescale DFO-2006 (Kawamura et al., 2007). In total, the age uncertainties range from 3.0 ka to 19.0 ka for the 7 IRHs.

https://doi.org/10.5194/tc-2023-35
Preprint. Discussion started: 16 March 2023

The Cryosphere Discussions
Open Access
EGU

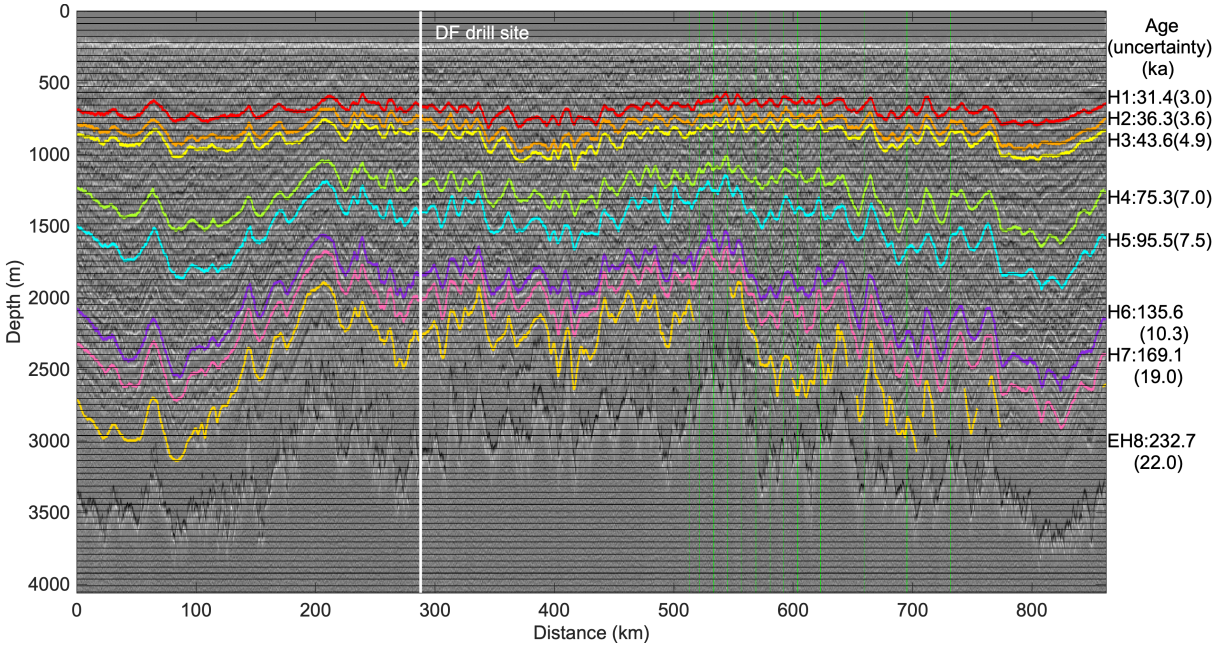

Figure 2. Radargram of the profile 20170240. Vertical white line shows the location of the DF drill site. Lines with different colours represent continuous horizons H1–H7 and specially traced discontinuous horizon EH8. The dated age and age uncertainty of each horizon is marked on the right.

2.4 1-D age model

To extrapolate the age–depth profile in the study area below the depth of the deepest IRH, we use a 1-D pseudo-steady ice flow model developed by Parrenin et al. (2006, 2017) but with a simplified constraint. This model assumes that the geometry, the shape of the vertical velocity profile and the relative density profile are constant. The real ice age χ can be calculated from the steady age $\bar{\chi}$ and the temporal factor $r(t)$ by

$$\bar{\chi} = \int_0^t r(\chi')\mathrm{d}\chi', \tag{1}$$

where $r(t)$ is deduced from the accumulation record of the DF ice core,

$$r(t) = \dot{a}(x,t)/\bar{a}(x), \tag{2}$$

where $\dot{a}$ is accumulation rate and $\bar{a}(x)$ is the temporally averaged accumulation rate at a certain point x. The steady age $\bar{\chi}$ can be inverted from depth d and the layer thickness $\lambda(d)$,

$$\bar{\chi}(d) = \int_0^d \frac{1}{\lambda(d')}\mathrm{d}d'. \tag{3}$$

https://doi.org/10.5194/tc-2023-35
Preprint. Discussion started: 16 March 2023

Assuming that there is no basal melt, $\lambda(d)$, approximated by the Lliboutry model (Lliboutry, 1979), is

$$\lambda(d) = \bar{a}\left(1 - \frac{p+2}{p+1}\left(\frac{d}{H_m}\right) + \frac{1}{p+1}\left(\frac{d}{H_m}\right)^{p+2}\right), \tag{4}$$

where H_m is the mechanical ice thickness, which means the effective ice thickness above the stagnant ice, and p is a shape factor controlling vertical deformation (Lilien et al., 2021).

We use a least square optimization to deduce the age–depth profile by varying $\dot{a}$, H_m and p. The main difference between the model we use here and the one developed by Parrenin et al. (2006) is that we use the mechanical ice thickness H_m instead of a term for the basal thermal conditions. Thus, no thermal modeling and boundary conditions are considered here. Instead, we use the inverted H_m to judge if there melting is present or if stagnant ice prevails. When H_m is greater than the observed ice thickness H we have melting conditions at the base. Otherwise, there is a basal layer of stagnant ice. If the basal ice is melting, the melt rate m can be obtained by

$$m = \lambda(H_{obs}), \tag{5}$$

where H_{obs} is the observed ice thickness. To quantify the reliability of the model at each point, we introduced a reliability index, i.e., the standard deviation of residuals, σ_R

$$\sigma_R = \sqrt{\frac{R^T r}{n_{iso}}}, \tag{6}$$

where n_{iso} is the number of IRHs, r is the residuals deduced by the age of IRHs χ_{iso} and modelled age χ_{mod}

$$R = \frac{\bar{\chi}_{iso} - \bar{\chi}_{mod}}{\sigma_{\chi_{iso}}}. \tag{7}$$

In this way the model achieves the balance of efficiency and numerical requirements. More details on the model can also be found in the companion paper (Chung et al., submitted).

3 Results

Age, age uncertainty of IRHs and temporal variations of accumulation rates at the DF drill from Dome Fuji Ice Core Project Members (2017) are used as input to the 1-D steady-state ice flow model. The outputs of the model are accumulation rate $\dot{a}$, shape factor p, mechanical thickness H_m, age–depth distribution and either basal melt rate or the thickness of the stagnant ice layer.

3.1 Modeling results for an exemplary profile

We integrate 1-D modeling results every 1 km along the exemplary the profile 20170240, displayed as a cross section through the ice sheet in Fig. 3, to get the 2-D modelled age–depth distribution. We find ice older than 1 Ma from $\sim$ 150 km to $\sim$ 550 km, where the ice sheet is relatively thin. Basal melting is present at the DF drill site and along most parts of the profile, where the mechanical ice thickness H_m (purple dash line) is larger (deeper) than the observed ice thickness (black line).

https://doi.org/10.5194/tc-2023-35
Preprint. Discussion started: 16 March 2023

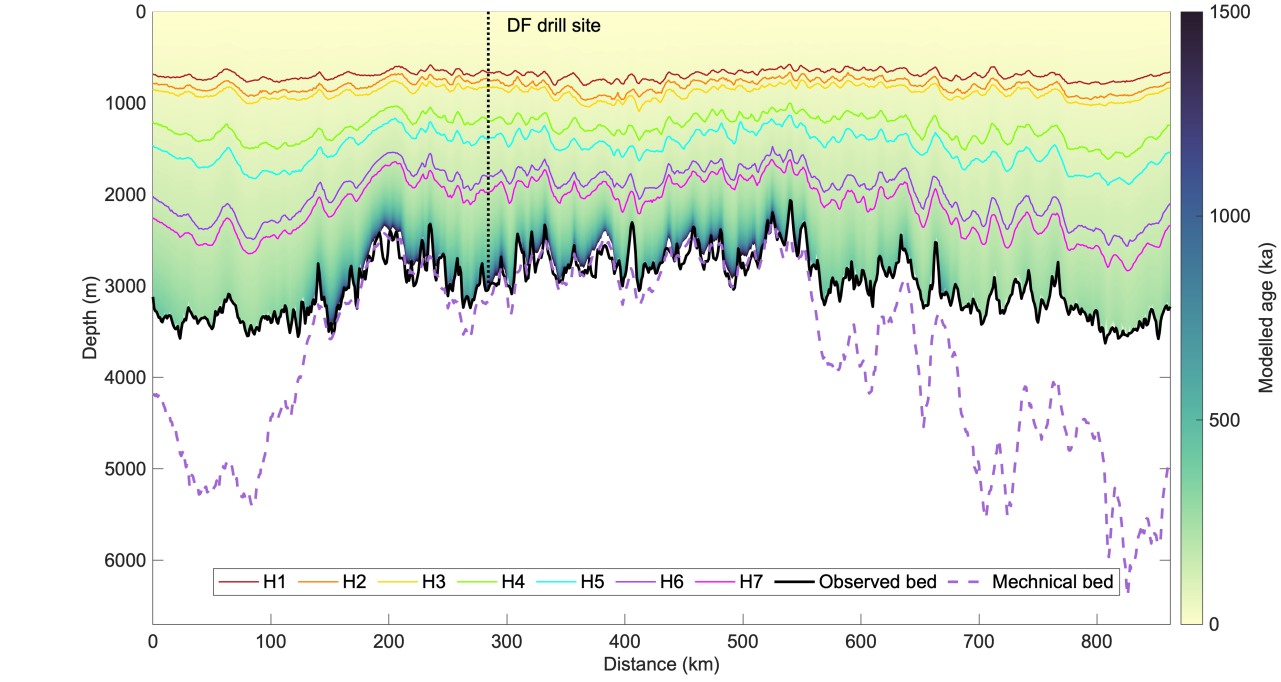

Figure 3. Modelled age–depth distribution of the radar profile 20170240. The coloured lines correspond to the traced IRHs shown in Fig. 2. The purple dashed line shows the mechanical ice thickness H_m and the black line shows the bed observed in the radargram. Where the purple dashed line is above the black line, stagnant ice is present and the depth difference between the two lines is the thickness of stagnant ice layer. In other cases, melting prevails.

3.2 Age of basal ice

We use 20 ka m^{-1} as a cut-off value for age density of basal ice, beyond which usage of proxies in the ice for paleoclimate reconstruction is currently difficult. This age density corresponds to a full 40 ka climate cycle in 2 m of ice. Fig. 4a shows the age of the basal ice (i.e. at the depth of the bed or where the age density reaches 20 ka m^{-1}) in the DF region. It varies from 215 ka to 2530 ka. Fig. 4b shows the corresponding depth of the basal ice, which falls in a depth range of 1.6–3.8 km. The age of the basal ice at the DF drill site is extrapolated as 1345.8±494.3 ka.

The age density of ice at 1.5 Ma is shown in Fig 5a, with a range of 6–20 ka m^{-1}. This figure also points out the four candidate areas where ice of more than 1.5 Ma old could potentially be found: the first one is a large subglacial mountain range located ∼100 km around the DF drill site; the second one is ∼ 160 km to the north-west of the DF drill site, connected with the first site; the third one is ∼ 240 km to the north-west of the DF drill site; the fourth one is ∼ 260 km to the south-west of the DF drill site. These fourth potential target areas are all situated in regions with ice thickness of 2200–3000 m, where the ice is not too thick, which would result in basal melting, but still thick enough to include the long-term and sufficiently resolved

https://doi.org/10.5194/tc-2023-35
Preprint. Discussion started: 16 March 2023

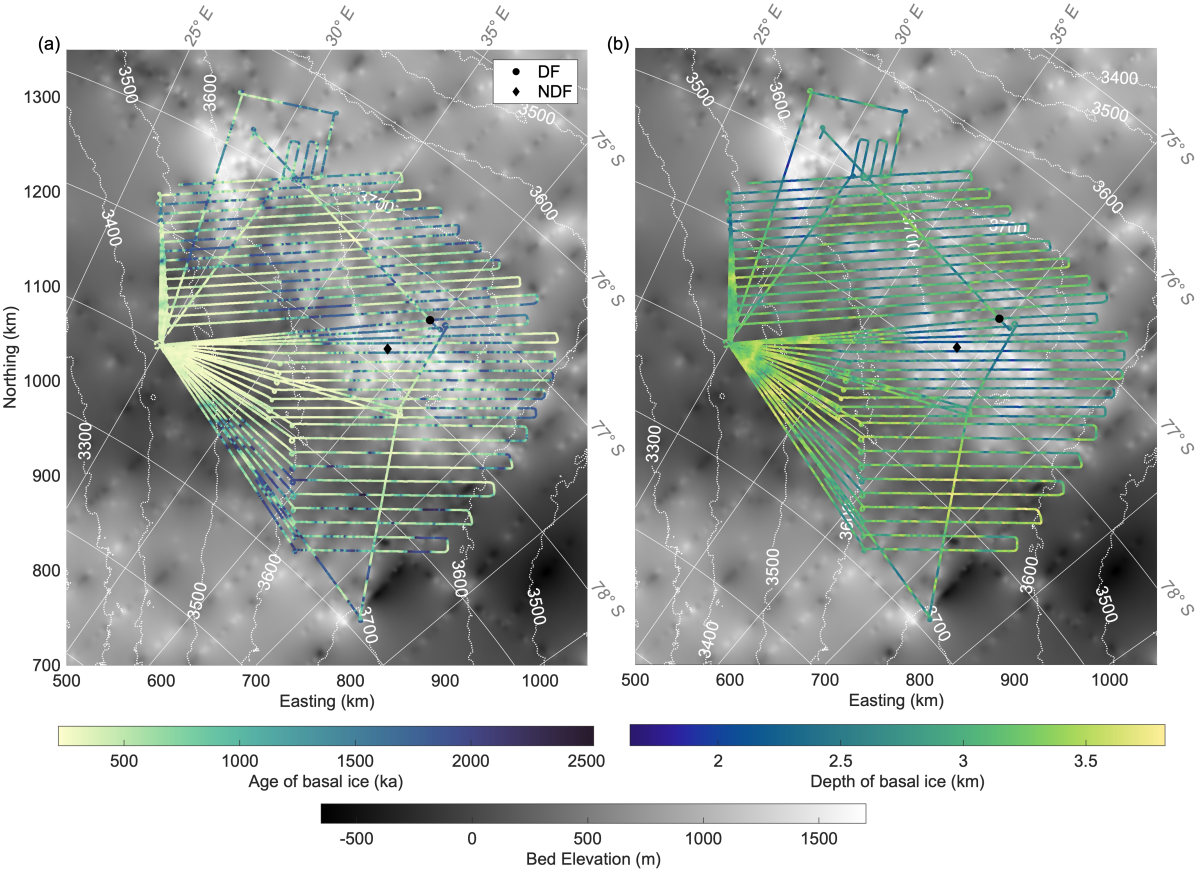

Figure 4. (a) Modelled age of the basal ice at a maximum age density of 20 ka m^{-1}. (b) Depth of the basal ice at an age density of 20 ka m^{-1}.

ice record. Moreover, these sites, especially the first one close to DF, appear to be distributed along some sort of high plateaus. This could imply that the ice column here is potentially less disturbed and includes layers of higher lateral continuity.

3.3 Basal thermal states

Basal condition is a crucial criterion for the presence of old ice, because any melting causes ice-loss in the lowermost part of the ice column, which severely limits the age of the basal ice (Fischer et al., 2013). From our model we also get the basal conditions, including melt rate or stagnant-ice thickness (Fig. 6a). According to our results, basal melting prevails over stagnant ice in the survey area. Modelled basal melt rates vary from 0 to 8.40 mm a^{-1}. Melting is significant $\sim$ 200 km west and $\sim$ 150 km south of DF, where we observe ice thicker than 3000 m, i.e. ice thick enough for the temperature to reach the pressure melting point. The basal melt rate at the DF drill site is interpolated as 0.11$\pm$0.37 mm a^{-1}. Stagnant ice has a thickness range of 0–400 m. Two clusters of stagnant ice are distributed $\sim$ 60 km south-west (around NDF) and $\sim$ 180 km north-west of the DF (in the

https://doi.org/10.5194/tc-2023-35
Preprint. Discussion started: 16 March 2023

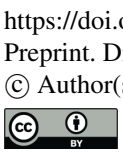

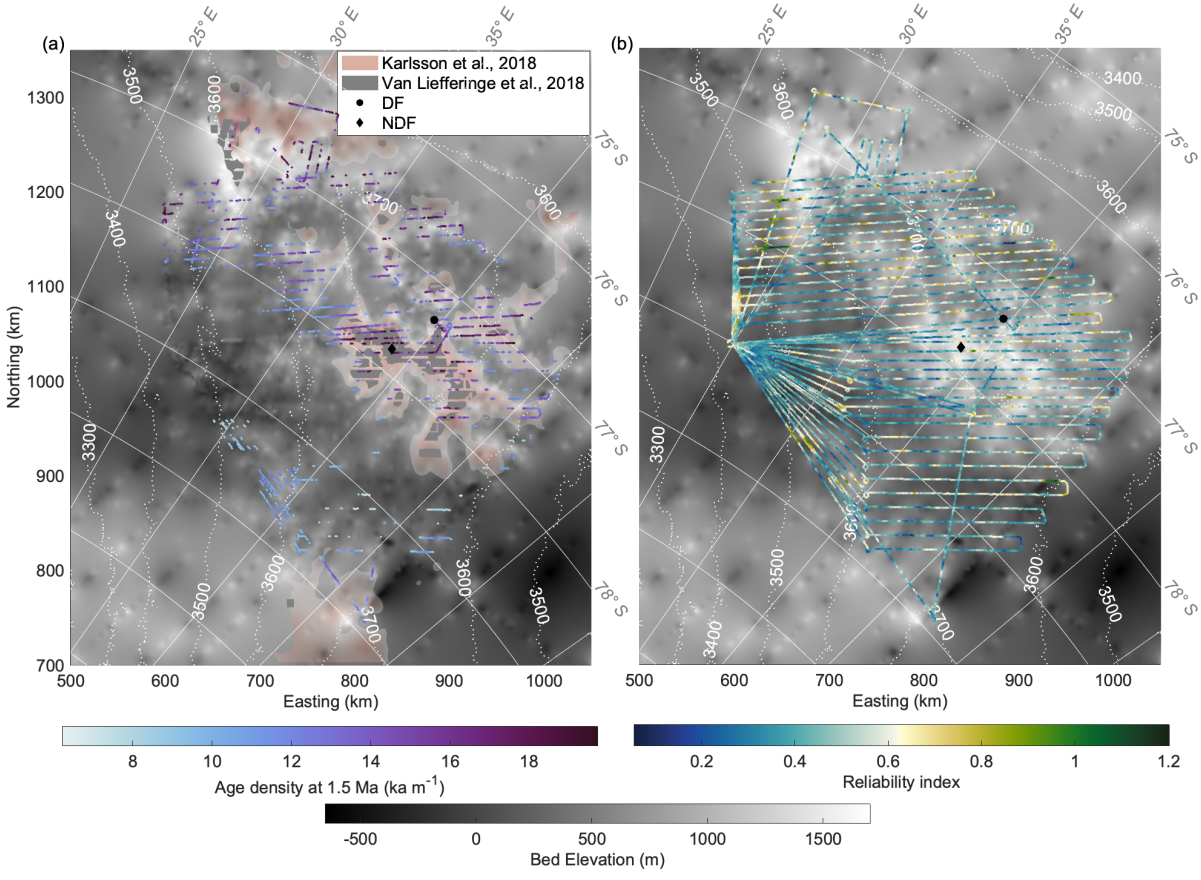

Figure 5. (a) Age density of ice at 1.5 Ma. Semi-transparent pink-red colored shades show potential old-ice sites suggested by Karlsson et al. (2018)—the deeper the color is, the higher the possibility of old ice. The gray shades show the old ice site suggested by Van Liefferinge et al. (2018). (b) Reliability index map in the DF region, the reliability of model decreases with reliability index increasing.

second old ice candidate). Our results show that melt rates are generally higher in subglacial basins and lower (or even frozen conditions) in subglacial mountainous terrain.

3.4 Accumulation rate

Accumulation rate is another important factor for the age distribution. We show temporally averaged (over 720 ka) accumulation rates in the DF region from our model results in Fig. 6b, they vary from 0.015 to 0.038 m a^{-1} ice equivalent. At the DF drill site, the accumulation rate spatially interpolated between the radar lines is 0.022 m a^{-1}. In the large DF region, it shows a north–south decreasing gradient.

In the Supplement Fig. S1 we also show the shape factor map in the DF region obtained from the model.

https://doi.org/10.5194/tc-2023-35
Preprint. Discussion started: 16 March 2023

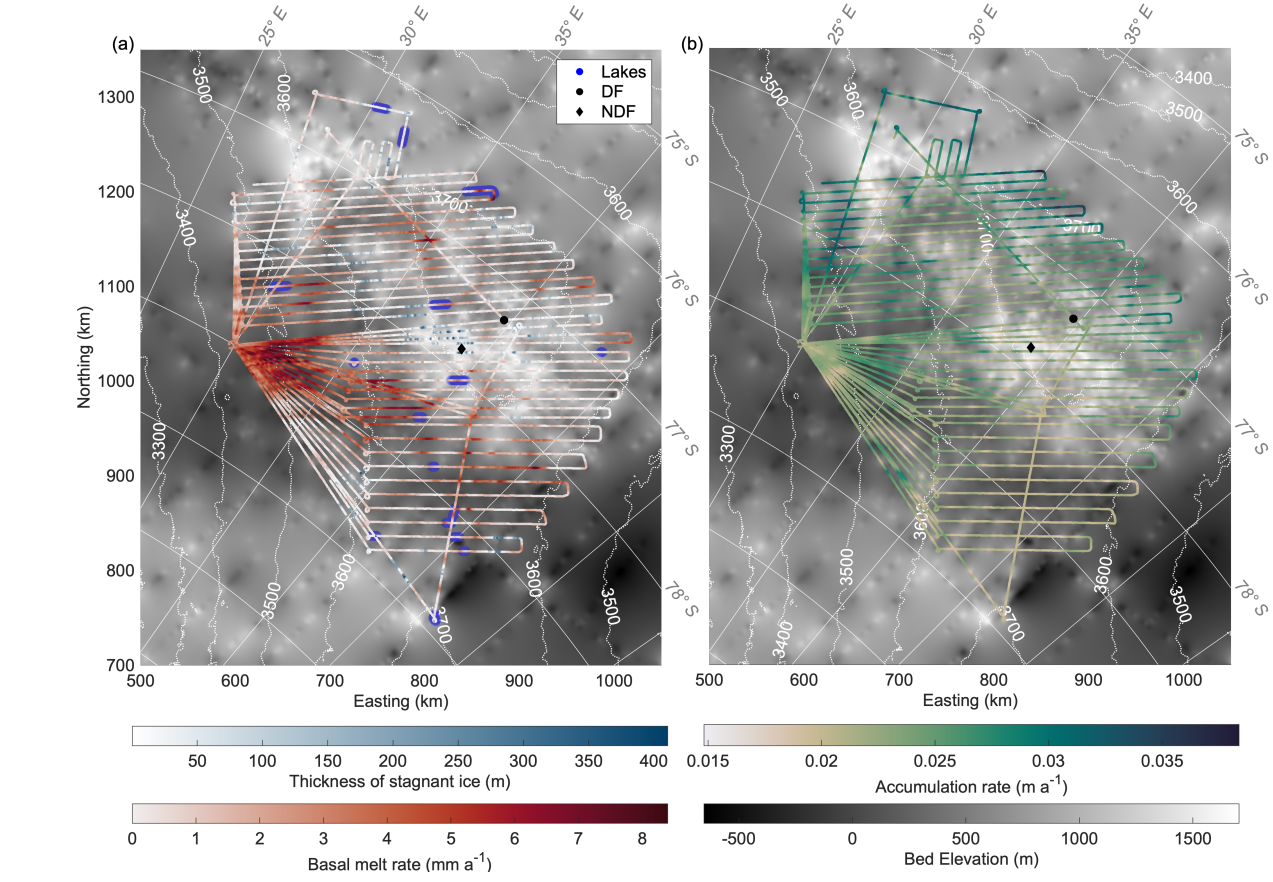

Figure 6. (a) Modelled stagnant-ice thickness and basal melt rate along the profiles of the radar survey: blue represents stagnant ice thickness and red represents the melt rate. Dark blue lines are subglacial lakes deduced from basal reflectivity in radargrams by Karlsson et al. (2018). (b) Modelled averaged accumulation rate in ice equivalent along the profiles of the radar survey.

4 Discussions

4.1 Age of ice: comparison with previous studies

Several previous studies have already investigated the potential age of basal ice either at the DF drill site or its surrounding region. At the DF drill site, Parrenin et al. (2007) proposed that ice more than several million yeas old could exist near the ice–bed interface according to the results of a 1-D ice flow model. Hondoh et al. (2002) deduced chronologies of the DF ice core based on the correlation between the local metronomic signal (Milankovitch components of the past surface temperature oscillations) and isotope record, and extropolated this timescale to 3050 m depth by a simplified ice-flow model. Their result suggested that age may reach 2000 ka at about 3000 m depth at the DF drill site. These two results correspond approximately to our inverted bottom age of 1345.8±494.3 ka at 3034.1 m.

https://doi.org/10.5194/tc-2023-35
Preprint. Discussion started: 16 March 2023

Obase et al. (2022) used a 1-D ice flow model, which computes the temporal evolution of the vertical age and temperature profiles. They also extended their modeling results along a DF–NDF radar transect from DF to NDF, where the basal ice has a tendency to be older. They used ground-based radar data from the JARE59 survey (2017–2018) in an area of approximately 120 km × 100 km, collected in a dense grid by an incoherent pulse-modulated VHF radar sounder with a peak transmission power of 1 kW, transmitter pulse widths of 60 ns and 250 ns, which corresponds to a pulse-limited vertical resolution of 5 and 21 m, respectively. In addition, the model they used is a transient model considering age and temperature both change with time. It estimates the age through the vertical advection equation, and uses the GHF as the basal boundary condition, while we use a 1-D steady model, which calculates the age through an analytical thinning function and excludes all thermal modeling by introducing a mechanical ice thickness.

Despite the differences in the radar data characteristics of the JARE59 and AWI surveys and slightly different models, the results are reasonably consistent. We estimate the age of the ice at DF to be 841.8 ka and 1034.5 ka at 100 m and 50 m above the bed, respectively, while Obase et al. (2022) extrapolated them as 880 ka and 1250 ka, respectively. In addition, our results confirm that the age of the basal ice is getting older from DF to NDF.

The two previous studies by Karlsson et al. (2018) and Van Liefferinge et al. (2018) are based on a thermodynamical model, considering regions with an ice flow velocity smaller than 1 m a^{-1}. Their main constraint for the presence of old ice is that the GHF is not sufficiently large to cause temperate conditions at the base, and thus melting. Another criterion is ice thicker than 2000 m and 2500 m respectively. Our approach, in contrast, is solely based on the observed age–depth distribution, which is then extrapolated to larger depth by using observed accumulation rates and making assumptions about the thinning function. The semi-transparent shades in Fig. 5a show the potential areas with old ice, suggested by Karlsson et al. (2018) and Van Liefferinge et al. (2018). The shades are to a large degree concurrent to our results, especially to the first candidate (a large subglacial mountain range located immediately around the DF drill site), although the approaches are very different.

4.2 Basal thermal state and accumulation rate: comparison with previous studies

A spatial comparison between our result and subglacial lakes identified previously by Karlsson et al. (2018) in Fig. 6a shows that we find all 16 lakes are located in regions where we obtain basal melting, and in 11 lakes we can observe significant melting.

Basal melt rate is a parameter impacted by the spatial distribution of GHF, which is a regional value and also can show strong variations on the local scale, depending on topography (Colgan et al., 2021). Regarding the local characteristic of GHF, we calculate regionally averaged melt rates in different areas around the DF drill from our results for the comparison with previous basal melt rate at DF. In our result, mean basal melt rates increase with the further distance to the DF site (i.e., in a larger region).

At the DF site, Parrenin et al. (2007) suggested that with a probability of 90 % the basal melt rate is smaller than 0.2 mm a^{-1} through 1D ice flow model. Seddik et al. (2011) deduced a basal melt rate of $\sim$ 0.35 mm a^{-1} assuming a GHF of 60 mW m^{-2}. Obase et al. (2022) got the conclusion of no melting for a GHF < 56 mW m^{-2}. These three results all agree with our mean basal melt rate of 0.16$\pm$0.37 mm a^{-1} within 5 km around DF. Obase et al. (2022) also simulated a basal melt rate changing

https://doi.org/10.5194/tc-2023-35
Preprint. Discussion started: 16 March 2023

from 1 to 1.5 mm a^{-1} for a GHF increasing from 57 to 58 mW m^{-2}, which corresponds with our averaged basal melt rate of 1.36±0.69 mW m^{-2} within 200 km around the DF site. Talalay et al. (2020) estimated a basal melt rate of 2.5±0.5 mm a^{-1} at the DF based on the temperature profile from the ice-core borehole and applying an analytical solution to infer the vertical velocity. This value is consistent with our mean basal melt rate of 1.67±0.76 mm a^{-1} in the entire DF region. However, this value is very different from our estimate at the DF drill site and probably closer to reality. In Section 4.3.3 we discuss the possibility of overestimation of the age of the basal ice due to the inflection point at the bottom part of the timescale, and therefore we may underestimate the basal melting. We show the detailed mean value and standard deviation of the basal melt rates within different distances to the DF drill in Fig. S2.

In the large DF region, the stagnant ice is present in only 8 % of the area along the radar profiles, and has an average thickness of 95.6 m. The distribution of the stagnant ice implies that the region immediately north of NDF is the area most likely to have a cold bed which could hold old ice in the DF region. Our companion paper shows in the DC region and LDC region, the basal thermal states are very different. Stagnant ice prevails over melting in the DC area and it dominates the LDC region, with a thickness of up to 250 m (Chung et al., submitted). The relatively warm basal thermal condition in the DF region is a negative factor for holding the old ice.

In the DF region, Fujita et al. (2011) showed an map of accumulation rate with a decreasing trend from 76° S to 78° S, which is consistent with the distribution of accumulation rate in our result.

4.3 Reliability and sensitivity study of the 1-D model

4.3.1 Reliability of the model

Our 1-D model does not consider horizontal advection, which although low near an ice divide, exists away from the divide. In these places, the reliability of the model could be relatively lower. We show the reliability index in the DF region (Fig. 5b). A smaller reliability index represents higher reliability of the model. The reliability index ranges from 0.1 (reliable) to 1.2 (less reliable) in the DF region. We find that in the northern part of the DF region, the model is relatively less reliable. The distribution indicates a relatively high reliability in the DF region compared to that in the DC region (0–2) (Chung et al., submitted). The reliability of the model in the DF could be overestimated because of the limited number and depth of IRHs.

To evaluate the reliability of the model results in ice deeper than the available IRHs, we also determine the spatial deviation of the age of basal ice in different distances to the DF/NDF as a function of normalized ice thickness. The spreading of the age of basal ice, shown in Table 1, generally increases with distance from DF/NDF, except between 100 and 200 km distance from both and >200 km from NDF. We interpret the larger spread to reflect the increasing transition from a dome-flow to a flank-flow regime. Within the region of clear characteristic of divide flow implies that it is reasonably adequate to apply a 1-D model. Our approach is comparable to the constraint mentioned above used by Karlsson et al. (2018) and Van Liefferinge et al. (2018) to investigate the age in areas with an ice flow velocity < 1 m a^{-1} (in ice equivalent). The standard deviation in age 5 km around NDF (47.9 ka) is much smaller than that around DF (392.3 ka), which could tentatively be interpreted as flow

https://doi.org/10.5194/tc-2023-35
Preprint. Discussion started: 16 March 2023


The Cryosphere Discussions
Open Access
EGU

Table 1. Spatial standard deviation of age of basal ice in different distances to DF and NDF.

	Standard deviation (ka)	
Distance (km)	Around DF	Around NDF
< 5	392.3	47.9
5–15	486.9	368.2
15–50	526.0	528.8
50–100	530.5	545.0
100–200	497.0	517.0
> 200	534.2	534.7

characteristics near NDF being closer to divide flow than those at DF. We show the distribution of the age–normalized depth in Fig. S3 to evaluate the flow regime further.

We then design sensitivity studies to investigate how different inputs affect the model and how the reliability of the model could be improved.

4.3.2 Sensitivity study

The thinning function and the normalized age–depth scale have a stronger gradient in deeper ice than at shallower depths, therefore the deepest horizon as well as the underlying age–depth scale may have an effect on our modeling result, including shape factor p, accumulation rate $\dot{a}$, mechanical ice thickness H_m, and age of basal ice χ_b. To investigate either effect we perform two sensitivity experiments for the profile 20170240. Our first run corresponds to our standard model run (STD) we have been discussing so far, i.e. it uses six or seven IRHs tracked and DFO2006+AICC2012 as the timescale. The timescale provides the information of the age of the IRHs and temporal variations of accumulation rates at DF. The second model run (RUN II) investigates the impact of different numbers of traced IRHs. In order to extend our available age–depth scale to larger depth, an extra discontinuous eighth horizon, EH8 with an age of 232.7 ka, is traced (Fig. 2). As this IRH is discontinuous in the study region, it could not be used reliably on all other profiles. In the third run (RUN III), we analyze how different timescales influence the modeling result. We use DFGT-2006 to replace DFO2006+AICC2012. DFGT-2006 is the timescale which reconstruct the age of ice above bed by a 1-D flow model based on the first DF ice core (Parrenin et al., 2007). Since the temporal variations of accumulation rates below 2503 m (the depth of the first deep ice core) in DFGT-2006 were derived from marine cores, which are not reliable, we use the temporal variations of accumulation rates below 2503 m from timescale DFO2006+AICC2012 as a replacement. We use the agescale with the seven IRHs from the standard run.

We provide statistic values of relative percentage difference of shape factor Δp %, accumulation rate $\Delta\dot{a}$, mechanical ice thickness ΔH_m, and age of basal ice $\Delta\chi_b$ along the profile 20170240 between STD and RUN II, STD and RUN III in Table 2, respectively, to quantify the difference between model results from different runs.

https://doi.org/10.5194/tc-2023-35
Preprint. Discussion started: 16 March 2023

Table 2. Mean value and standard deviation of relative percentage difference between model runs for the profile 20170240.

	$\Delta\chi_b$ %		Δp %		$\Delta\dot{a}$ %		ΔH_m %	
	Mean	Std. dev.	Mean	Std. dev.	Mean	Std. dev.	Mean	Std. dev.
STD–RUN II	14.58	14.69	12.55	10.07	0.83	0.71	4.35	3.34
STD–RUN III	10.35	10.71	9.07	6.09	3.11	0.18	3.15	0.60

The age of the basal ice and the shape factor are affected severely by an extra IRH with mean Δp % of 12.55 % and mean $\Delta\chi_b$ % of 14.58 %. In some regions, EH8 has a somewhat different shape with the uppermost seven IRHs and thus largely changes the inversion of shape factor and thinning function of every 1-D model, which will lead to significant change of age of basal ice. Between STD and RUN III, the mean relative difference of age of the basal ice and the shape factor are also large (10.35 % and 9.07 %), they prove the importance of using the most reliable timescale of the ice core. Without the impact of the EH8, the standard deviation of Δp % and $\Delta\chi_b$ % are still significant (6.09 % and 10.71 %), which could be relevant to the changes in subglacial topography.

$\Delta\dot{a}$ % between STD and RUN II/RUN III has a mean value of 0.83 % and 3.11 %, respectively, which implies the accumulation rate is almost unaffected by adding an extra IRH and affected more by the timescale. The standard deviation of $\Delta\dot{a}$ % between STD and RUN III is low (0.18 %), proves the relative difference is stable along the profile. So using different temporal variations of accumulation rates at DF could be the main reason for the difference of modeled accumulation rate between STD and RUN III. This is, however, not surprising, as accumulation is more influenced by changes in the near-surface regions and less by changes at large depths (e.g. an additional constraining IRH) (Sutter et al., 2021).

Mean values of the relative change in the mechanical ice thickness ΔH_m imply that both the number of IRHs (4.35 %) and change of agescale (3.15 %) have a comparatively small impact on the deduced mechanical ice thickness, which means that the mechanical ice thickness obtained from our model is relatively robust compared to other quantities.

We show and analyse the model results for all three runs in Fig. S4 and relative percentage difference of model results between STD and RUN II/RUN III in Fig. S5.

4.3.3 Comparison of the age–depth scales

Comparing the age–depth distribution at the DF drill of the three model runs (Fig.7), we find that at depths above $\sim$ 2500 m, the three runs have very similar age–depth scales.

The difference between STD and RUN II/RUN III are much larger below a depth of 2500 m, where STD has an age of basal ice of 1345.8$\pm$494.3 ka, RUN II has an extra layer and a resulting age of the basal ice of 1956.1$\pm$716.8 ka, RUN III uses input from a different timescale and obtains an age of 1933.7$\pm$751.9 ka at the ice–bed interface. This comparison shows that both, the number of IRHs and the agescale, have a significant influence on age of the basal ice.

https://doi.org/10.5194/tc-2023-35
Preprint. Discussion started: 16 March 2023

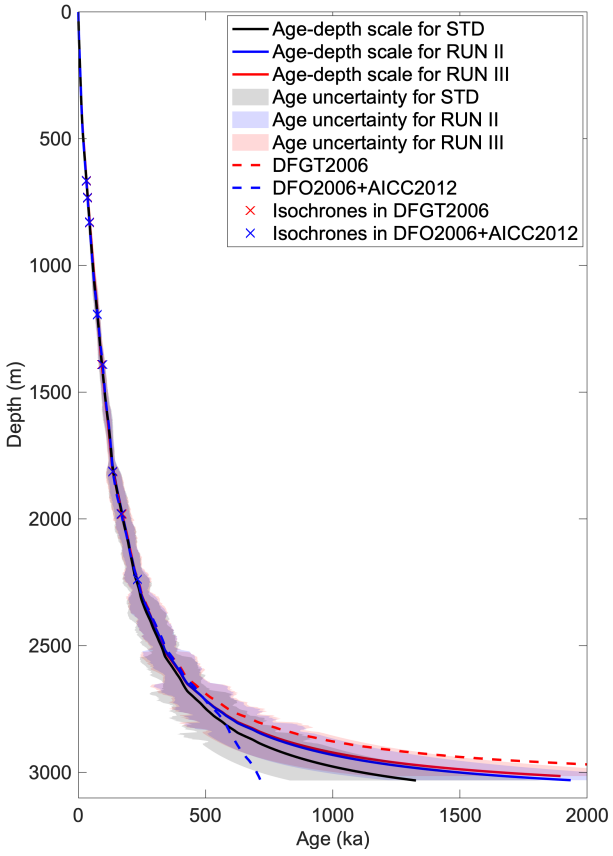

Figure 7. Comparison of age–depth scales of three models (solid lines), their uncertainties (shades) and two timescales from the DF ice core (dashed line). The crosses show the age and depth of IRHs.

Comparing the modeling result of STD and RUN II with their timescale from the DF ice core (DFO2006+AICC2012), we find that above ∼ 2300 m, both modeling results have good correspondence with the timescale. From ∼ 2300 m to ∼ 2750 m, only the RUN II agrees with DFO2006+AICC2012. Below ∼ 2750 m, modeled age keeps the exponential relation with depth but the real timescale DFO2006+AICC2012 starts deviating from it. Thus, modeled age has a much larger age gradient in the same depth range, which leads to an overestimation by a factor of two of the age of basal ice at this case. This implies deeper IRHs below 2750 m at this case will have a positive impact on the modeling result as they can provide important real-age constraints for the model. Considering the overestimation we observe at the DF drill, the reliability of our model is probably overestimated. Whether the inflection point in the age–depth profile is a general feature in the DF region is still an open question.

https://doi.org/10.5194/tc-2023-35
Preprint. Discussion started: 16 March 2023

4.3.4 Limitations of radar system

According to the sensitivity study and comparison of age–depth scales, the shape of IRHs (i.e., the accuracy of tracing) and the depth of IRHs have significant impacts on the modelled age of the ice. However, compared to modern state-of-the-art radar systems, the data collected with the AWI RES system has a lower resolution of 50 m, which leads to marked errors during manual IRHs picking and thus lower reliability of modeling results. In addition, although we pick the deepest continuous layer with an age of 169.1 ka in this study, there is still more than one third of the ice column in the lowermost part that is not dated. The lack of signal in lowermost part likely originates not only from ice dynamics but also from the limitations of the radar system. Rodriguez-Morales et al. (2020) showed the comparison of data collected by CReSIS' UWB radar, NIPR radar and our AWI's airborne RES system (600-ns burst) along semicoincident survey trajectories in the DF region. It implied that at the same depth modern systems would provide not only a higher resolution, but most likely also a deeper detection of continuous IRHs (Rodriguez-Morales et al., 2020).

Our sensitivity study also shows the correspondence between the age of basal ice and ice thickness, as a crucial input in the ice-flow model. Accurate ice thickness can improve the reliability of the modeling results. Our radar data was collected with an incoherent burst radar system, which means hyperbolic effects in signals are strong and affect the accuracy of subglacial topography. According to Tsutaki et al. (2022), the average difference between ice thickness observed from Japanese radar system (with high-gain and high-directivity antennae) and the AWI RES system is −8 m, and the standard deviation is 108 m. The high standard deviation implies the details of bed topography observed by two radar systems could be significantly different, which may cause the misalignment in modeling results.

5 Conclusions and perspectives

From the combination of observed internal layer stratigraphy with our 1D ice flow model We draw the following conclusions:

1. We identify four potential candidates for old ice in the DF region: a subglacial mountainous target located around the DF drill site with a radius of $\sim$ 100 km, $\sim$ 160 km to the north-west of the DF drill, $\sim$ 240 km to the north-west of the DF drill and $\sim$ 260 km to the south-west of DF drill. At the DF drill site, the age of ice is 841.8 ka and 1034.5 ka at 100 m and 50 m above the bed, and 1345.8 ka at the ice–bed interface.

2. Modelled basal melt rates vary from 0 to 8.4 mm a^{-1}, melting being significant $\sim$ 200 km west and 150 km south of the DF drill. Stagnant ice seems to be present mainly immediately north of NDF and $\sim$ 180 km north-west of the DF drill stie. It occupies only 8 % of the radar profiles with an average thickness of 95.6 m. The region close to NDF has the most favorable conditions of a cold bed for holding old ice. There is no stagnant ice at the DF site, the melt rate at the DF drill is 0.11 ± 0.37 mm a^{-1}. Compared to a thickness of stagnant ice of $\sim$ 200 m in the LDC region, the basal thermal condition in the DF region is warmer. We obtain an average accumulation rate over 720 ka of 0.015–0.038 m a^{-1} ice equivalent in the DF region and 0.022 m a^{-1} ice equivalent at the DF drill site.

3. An extra IRH at deeper depth and/or a different timescale significantly affect the model results. This underlines the importance of using IRHs traced as deep as possible and the most trustworthy timescale to get more reliable model results.

https://doi.org/10.5194/tc-2023-35
Preprint. Discussion started: 16 March 2023

Regarding our results, the age of basal ice could be overestimated in the DF region because of limitations in the depth of our IRHs and because of the inability of our model to capture complex thinning phenomena in the basal layer.

Our study still has some limitations which might be considered in future approaches. Our model does not consider horizontal advection and assumes that the basal sliding ratio is negligible, which are proper assumptions at DF. To improve the reliability of model results in regions further from DF, a basal sliding term could be added, but it will be difficult to infer at the same time the mechanical ice thickness, the velocity shape exponent and the sliding ratio. Furthermore, 3-D full stokes model can lift restrictions, however, there are still challenges for 3-D models, including heavy computation time, complicated boundary conditions and conjunction between 3-D model and age observations. Moreover, the radar system we use in the study limits the number, depth and accuracy of the IRHs traced and the resolution of bed topography observed in the radargrams, which both affect the modeling results. Using ground-based observations from improved radar systems with higher vertical as well as horizontal resolution in sub-regions of the larger DF area, as were already acquired in the past, will complement the large-scale results from our study.

Code availability. The model is available from Github. https://github.com/ailsachung/IsoInv1D

Data availability. We are waiting for the raw radar data and IRHs traced in radargrams being available on data repository. The bed elevation and surface elevation dataset collected in the NASA Making Earth System Data Records for Use in Research Environments (MEaSUREs) program (Morlighem et al., 2017, 2020) are available on https://nsidc.org/data/nsidc-0756/versions/3. We call elevation data through Antarctic Mapping Tools in MATLAB on https://de.mathworks.com/matlabcentral/fileexchange/47638-antarctic-mapping-tools (Greene et al., 2017). The ice thickness observed from radar data are published on https://doi.org/10.1594/PANGAEA.891323 (Karlsson et al., 2018).

Author contributions. OE coordinated the BE–OI project and designed this study. ZW carried out experiments and wrote the manuscript with input from all co-authors. ZW and DS processed, traced the radar isochrones. FP developed the model. AC improved and adapted the model to the conditions at Dome Fuji. JF drilled the B53 ice core and provided depth–density profile of the ice core. All coauthors read and commented on the manuscript.

Competing interests. O.E. is an edtior of The Cryosphere. The authors declare no other competing interests.

Acknowledgements. This publication was generated in the frame of Beyond EPICA-Oldest Ice (BE-OI). The project has received funding from the European Union's Horizon 2020 research and innovation programme under grant agreement No. 730258 (BE-OI CSA). It has received funding from the Swiss State Secretariate for Education, Research and Innovation (SERI) under contract number 16.0144. It is fur-

https://doi.org/10.5194/tc-2023-35
Preprint. Discussion started: 16 March 2023

thermore supported by national partners and funding agencies in Belgium, Denmark, France, Germany, Italy, Norway, Sweden, Switzerland, the Netherlands, and the United Kingdom. Logistic support is mainly provided by AWI, BAS, ENEA and IPEV. The opinions expressed and arguments employed herein do not necessarily reflect the official views of the European Union funding agency, the Swiss Government, or other national funding bodies. We thank the logistics field team and flight crew for support during the expedition. We thank Emerson E&P Software, Emerson Automation Solutions, for providing licenses in the scope of the Emerson Academic Program. We thank Brice Van Liefferinge for providing the locations of the promising old ice in the DF region in his previous study. We thank Nanna B. Karlsson, who offered the detailed locations of the subglacial lakes and the old ice candidates in her previous study. We thank Kenji Kawamura for the insightful discussions on the DFO2006+AICC2012 timescale of the Dome Fuji ice core. Zhuo Wang is funded by China Scholarship Council (No. 202106170102). Thank Professor Zhaofa Zeng for supporting her in getting the grant and jointly studying abroad as her supervisor in Jilin University. Ailsa Chung is funded through the DEEPICE project, from the European Union's Horizon 2020 research and innovation programme under the Marie Sklodowska-Curie grant agreement No. 955750.

https://doi.org/10.5194/tc-2023-35
Preprint. Discussion started: 16 March 2023

References

Ageta, Y., Azuma, Y., Fujii, Y., Fujino, K., Fujita, S., Furukawa, T., Hondoh, T., Kameda, T., Kamiyama, K., Katagiri, K., et al.: Deep ice-core drilling at Dome Fuji and glaciological studies in east Dronning Maud Land, Antarctica, Annals of Glaciology, 27, 333–337, 1998.

Cavitte, M. G., Blankenship, D. D., Young, D. A., Schroeder, D. M., Parrenin, F., Lemeur, E., Macgregor, J. A., and Siegert, M. J.: Deep radiostratigraphy of the East Antarctic plateau: connecting the Dome C and Vostok ice core sites, Journal of Glaciology, 62, 323–334, 2016.

Chung, A., Parrenin, F., Steinhage, D., Mulvaney, R., Martin, C., Cavitte, M., Lilien, D., Helm, V., Taylor, D., Gogineni, P., Ritz, C., Frezzotti, M., O'Neill, C., Miller, H., Dahl-Jensen, D., and Eisen, O.: Stagnant ice and age modelling in the Dome C region, Antarctica, submitted.

Colgan, W., MacGregor, J. A., Mankoff, K. D., Haagenson, R., Rajaram, H., Martos, Y. M., Morlighem, M., Fahnestock, M. A., and Kjeldsen, K. K.: Topographic correction of geothermal heat flux in greenland and antarctica, Journal of Geophysical Research: Earth Surface, 126, e2020JF005 598, 2021.

Dome Fuji Ice Core Project Members, D. F. I. C. P. M.: State dependence of climatic instability over the past 720,000 years from Antarctic ice cores and climate modeling, Science advances, 3, e1600 446, 2017.

Fischer, H., Severinghaus, J., Brook, E., Wolff, E., Albert, M., Alemany, O., Arthern, R., Bentley, C., Blankenship, D., Chappellaz, J., et al.: Where to find 1.5 million yr old ice for the IPICS" Oldest-Ice" ice core, Climate of the Past, 9, 2489–2505, 2013.

Freitag, J., Kipfstuhl, S., and Laepple, T.: Core-scale radioscopic imaging: a new method reveals density–calcium link in Antarctic firn, Journal of Glaciology, 59, 1009–1014, 2013.

Fujita, S., Maeno, H., Uratsuka, S., Furukawa, T., Mae, S., Fujii, Y., and Watanabe, O.: Nature of radio echo layering in the Antarctic ice sheet detected by a two-frequency experiment, Journal of Geophysical Research: Solid Earth, 104, 13 013–13 024, 1999.

Fujita, S., Holmlund, P., Andersson, I., Brown, I., Enomoto, H., Fujii, Y., Fujita, K., Fukui, K., Furukawa, T., Hansson, M., et al.: Spatial and temporal variability of snow accumulation rate on the East Antarctic ice divide between Dome Fuji and EPICA DML, The Cryosphere, 5, 1057–1081, 2011.

Fujita, S., Parrenin, F., Severi, M., Motoyama, H., and Wolff, E.: Volcanic synchronization of Dome Fuji and Dome C Antarctic deep ice cores over the past 216 kyr, Climate of the Past, 11, 1395–1416, 2015.

Greene, C. A., Gwyther, D. E., and Blankenship, D. D.: Antarctic mapping tools for MATLAB, Computers & Geosciences, 104, 151–157, 2017.

Hondoh, T., Shoji, H., Watanabe, O., Salamatin, A. N., and Lipenkov, V. Y.: Depth–age and temperature prediction at Dome Fuji station, East Antarctica, Annals of Glaciology, 35, 384–390, 2002.

Jouzel, J. and Masson-Delmotte, V.: Deep ice cores: the need for going back in time, Quaternary Science Reviews, 29, 3683–3689, 2010.

Kameda, T., Fujita, K., Sugita, O., Hirasawa, N., and Takahashi, S.: Total solar eclipse over Antarctica on 23 November 2003 and its effects on the atmosphere and snow near the ice sheet surface at Dome Fuji, Journal of Geophysical Research: Atmospheres, 114, 2009.

Karlsson, N. B., Binder, T., Eagles, G., Helm, V., Pattyn, F., Van Liefferinge, B., and Eisen, O.: Glaciological characteristics in the Dome Fuji region and new assessment for "Oldest Ice", The Cryosphere, 12, 2413–2424, 2018.

Karlsson, N. B., Binder, T., Eagles, G., Helm, V., Pattyn, F., Van Liefferinge, B., and Eisen, O.: Ice thickness from the Dome Fuji region, East Antarctica from ice-penetrating radar, https://doi.org/10.1594/PANGAEA.891323, 2018.

Kawamura, K., Parrenin, F., Lisiecki, L., Uemura, R., Vimeux, F., Severinghaus, J. P., Hutterli, M. A., Nakazawa, T., Aoki, S., Jouzel, J., et al.: Northern Hemisphere forcing of climatic cycles in Antarctica over the past 360,000 years, Nature, 448, 912–916, 2007.

https://doi.org/10.5194/tc-2023-35
Preprint. Discussion started: 16 March 2023

Lilien, D. A., Steinhage, D., Taylor, D., Parrenin, F., Ritz, C., Mulvaney, R., Martín, C., Yan, J.-B., O'Neill, C., Frezzotti, M., Miller, H., Gogineni, P., Dahl-Jensen, D., and Eisen, O.: Brief communication: New radar constraints support presence of ice older than 1.5 Myr at Little Dome C, The Cryosphere, 15, 1881–1888, 2021.

Lisiecki, L. E. and Raymo, M. E.: A Pliocene-Pleistocene stack of 57 globally distributed benthic δ^{18}O records, Paleoceanography, 20, 2005.

Lliboutry, L.: A critical review of analytical approximate solutions for steady state velocities and temperatures in cold ice-sheets, Z. Gletscherkde. Glazialgeol., 15, 135–148, 1979.

Morlighem, M., Williams, C. N., Rignot, E., An, L., Arndt, J. E., Bamber, J. L., Catania, G., Chauché, N., Dowdeswell, J. A., Dorschel, B., et al.: BedMachine v3: Complete bed topography and ocean bathymetry mapping of Greenland from multibeam echo sounding combined with mass conservation, Geophysical research letters, 44, 11–051, 2017.

Morlighem, M., Rignot, E., Binder, T., Blankenship, D., Drews, R., Eagles, G., Eisen, O., Ferraccioli, F., Forsberg, R., Fretwell, P., et al.: Deep glacial troughs and stabilizing ridges unveiled beneath the margins of the Antarctic ice sheet, Nature Geoscience, 13, 132–137, 2020.

Motoyama, H.: The second deep ice coring project at Dome Fuji, Antarctica, Scientific Drilling, 5, 41–43, 2007.

Motoyama, H., Takahashi, A., Tanaka, Y., Shinbori, K., Miyahara, M., Yoshimoto, T., Fujii, Y., Furusaki, A., Azuma, N., Ozawa, Y., et al.: Deep ice core drilling to a depth of 3035.22 m at Dome Fuji, Antarctica in 2001–07, Annals of Glaciology, 62, 212–222, 2021.

Nixdorf, U., Steinhage, D., Meyer, U., Hempel, L., Jenett, M., Wachs, P., and Miller, H.: The newly developed airborne radio-echo sounding system of the AWI as a glaciological tool, Annals of Glaciology, 29, 231–238, 1999.

Obase, T., Abe-Ouchi, A., Saito, F., Tsutaki, S., Fujita, S., Kawamura, K., and Motoyama, H.: A one-dimensional temperature and age modeling study for selecting the drill site of the oldest ice core around Dome Fuji, Antarctica, The Cryosphere Discussions, 2022, 1–24, 2022.

Parrenin, F., Hindmarsh, R., and Rémy, F.: Analytical solutions for the effect of topography, accumulation rate and lateral flow divergence on isochrone layer geometry, Journal of Glaciology, 52, 191–202, 2006.

Parrenin, F., Dreyfus, G., Durand, G., Fujita, S., Gagliardini, O., Gillet, F., Jouzel, J., Kawamura, K., Lhomme, N., Masson-Delmotte, V., et al.: 1-D-ice flow modelling at EPICA Dome C and Dome Fuji, East Antarctica, Climate of the Past, 3, 243–259, 2007.

Parrenin, F., Cavitte, M. G., Blankenship, D. D., Chappellaz, J., Fischer, H., Gagliardini, O., Masson-Delmotte, V., Passalacqua, O., Ritz, C., Roberts, J., et al.: Is there 1.5-million-year-old ice near Dome C, Antarctica?, The Cryosphere, 11, 2427–2437, 2017.

Raisbeck, G., Yiou, F., Cattani, O., and Jouzel, J.: 10Be evidence for the Matuyama–Brunhes geomagnetic reversal in the EPICA Dome C ice core, Nature, 444, 82–84, 2006.

Raymo, M. E., Lisiecki, L., and Nisancioglu, K. H.: Plio-Pleistocene ice volume, Antarctic climate, and the global δ18O record, Science, 313, 492–495, 2006.

Rodriguez-Morales, F., Braaten, D., Mai, H. T., Paden, J., Gogineni, P., Yan, J.-B., Abe-Ouchi, A., Fujita, S., Kawamura, K., Tsutaki, S., et al.: A Mobile, Multichannel, UWB Radar for Potential Ice Core Drill Site Identification in East Antarctica: Development and First Results, IEEE Journal of Selected Topics in Applied Earth Observations and Remote Sensing, 13, 4836–4847, 2020.

Saruya, T., Fujita, S., Iizuka, Y., Miyamoto, A., Ohno, H., Hori, A., Shigeyama, W., Hirabayashi, M., and Goto-Azuma, K.: Development of crystal orientation fabric in the Dome Fuji ice core in East Antarctica: implications for the deformation regime in ice sheets, The Cryosphere, 16, 2985–3003, 2022.

Seddik, H., Greve, R., Zwinger, T., and Placidi, L.: A full Stokes ice flow model for the vicinity of Dome Fuji, Antarctica, with induced anisotropy and fabric evolution, The Cryosphere, 5, 495–508, 2011.

https://doi.org/10.5194/tc-2023-35
Preprint. Discussion started: 16 March 2023

Singer, B. and Brown, L. L.: The Santa Rosa Event: 40Ar/39Ar and paleomagnetic results from the Valles rhyolite near Jaramillo Creek, Jemez Mountains, New Mexico, Earth and Planetary Science Letters, 197, 51–64, 2002.

Sun, B., Moore, J. C., Zwinger, T., Zhao, L., Steinhage, D., Tang, X., Zhang, D., Cui, X., and Martín, C.: How old is the ice beneath Dome A, Antarctica?, The Cryosphere, 8, 1121–1128, 2014.

Sutter, J., Fischer, H., and Eisen, O.: Investigating the internal structure of the Antarctic ice sheet: the utility of isochrones for spatiotemporal ice-sheet model calibration, The Cryosphere, 15, 3839–3860, 2021.

Talalay, P., Li, Y., Augustin, L., Clow, G. D., Hong, J., Lefebvre, E., Markov, A., Motoyama, H., and Ritz, C.: Geothermal heat flux from measured temperature profiles in deep ice boreholes in Antarctica, The Cryosphere, 14, 4021–4037, 2020.

Tsutaki, S., Fujita, S., Kawamura, K., Abe-Ouchi, A., Fukui, K., Motoyama, H., Hoshina, Y., Nakazawa, F., Obase, T., Ohno, H., Oyabu, I., Saito, F., Sugiura, K., and Suzuki, T.: High-resolution subglacial topography around Dome Fuji, Antarctica, based on ground-based radar surveys over 30 years, The Cryosphere, 16, 2967–2983, 2022.

Van Liefferinge, B. and Pattyn, F.: Using ice-flow models to evaluate potential sites of million year-old ice in Antarctica, Climate of the Past, 9, 2335–2345, 2013.

Van Liefferinge, B., Pattyn, F., Cavitte, M. G., Karlsson, N. B., Young, D. A., Sutter, J., and Eisen, O.: Promising Oldest Ice sites in East Antarctica based on thermodynamical modelling, The Cryosphere, 12, 2773–2787, 2018.

Watanabe, O., Kamiyama, K., Motoyama, H., Fujii, Y., Shoji, H., and Satow, K.: The paleoclimate record in the ice core at Dome Fuji station, East Antarctica, Annals of Glaciology, 29, 176–178, 1999.

Willeit, M., Ganopolski, A., Calov, R., and Brovkin, V.: Mid-Pleistocene transition in glacial cycles explained by declining CO2 and regolith removal, Science Advances, 5, eaav7337, 2019.

Winter, A., Steinhage, D., Arnold, E. J., Blankenship, D. D., Cavitte, M. G., Corr, H. F., Paden, J. D., Urbini, S., Young, D. A., and Eisen, O.: Comparison of measurements from different radio-echo sounding systems and synchronization with the ice core at Dome C, Antarctica, The Cryosphere, 11, 653–668, 2017.

Young, D. A., Roberts, J. L., Ritz, C., Frezzotti, M., Quartini, E., Cavitte, M. G., Tozer, C. R., Steinhage, D., Urbini, S., Corr, H. F., et al.: High-resolution boundary conditions of an old ice target near Dome C, Antarctica, The Cryosphere, 11, 1897–1911, 2017.